Journal of Power Sources 241 (2013) 61–69

Contents lists available at SciVerse ScienceDirect

Journal of Power Sources

journal homepage: www.elsevier.com/locate/jpowsour

Binding mechanism of sulfur and dehydrogenated polyacrylonitrile in sulfur/polymer composite cathode

The Nam Long Doan, Mahmoudreza Ghaznavi, Yan Zhao, Yongguang Zhang, Aishuak Konarov, Mikhail Sadhu, Ravichandra Tangirala, P. Chen*

Department of Chemical Engineering and Waterloo Institute for Nanotechnology, University of Waterloo, 200 University Avenue West, Waterloo, Ontario N2L3G1, Canada

HIGHLIGHTS

- Binding mechanism of sulfur and dehydrogenated polyacrylonitrile is proposed.
- C/H molar ratio is about 6 in the thermally stable structure.
- The upper limit for sulfur content in the composite is 56 wt%.
- Higher sulfur content will result in poor electrochemical performance.

ARTICLE INFO

Article history:
Received 2 March 2013
Received in revised form
11 April 2013
Accepted 24 April 2013
Available online 30 April 2013

Keywords:
Polyacrylonitrile
Lithium–sulfur battery
Sulfur content
Cathode
Composite

ABSTRACT

A composite consisting of sulfur/dehydrogenated polyacrylonitrile is one of the most promising cathode materials for use in rechargeable lithium–sulfur batteries. However, the reported sulfur contents have been low, less than 50 wt%, which compromise the intrinsic high specific capacity and energy of elemental sulfur and hence decrease significantly the specific energy of the composite. To identify the potential to further increase the sulfur content, we elucidate the binding mechanism of sulfur and polyacrylonitrile in their composite. The heat treatment experiments at varying timespans with excess sulfur showed a constancy of sulfur content after a critical length of timespan, indicating the saturation of sulfur in the structure of dehydrogenated polyacrylonitrile. Based on molecular structure and size consideration, it is proposed that the binding involves the formation of an 8 membered ring of sulfur embedded between 4 heterocyclic rings of dehydrogenated polyacrylonitrile. From this model and experimental results, we show that there exists an upper limit of sulfur content in the sulfur/dehydrogenated polyacrylonitrile composite at 56 wt%.

1. Introduction

The lithium-ion battery first introduced by Sony in 1991 is considered the most successful and most widely applied portable energy storage system. While specific energy of the battery has improved over time using more innovative cell design, the specific energy limit appears to have been reached [1,2]. Because the specific capacities of commercial cathode materials such as $LiCoO_2$, $LiFePO_4$, $LiMn_2O_4$ [2–5] (all less than 170 mA h g^{-1}) are no match for the current anode materials such as lithium (3861 mA h g^{-1}), silicon (4200 mA h g^{-1}) and even lithium intercalated graphite (372 mA h g^{-1}), cathode material appears to be a limiting factor for enhancing the specific energy of a battery [2]. From this consideration, it is obvious that cathode materials with higher specific capacities are required to improve the specific energy and enhance energy storage efficiency.

Of all known cathode materials, sulfur offers one of the highest theoretical specific capacities, 1672 mA h g^{-1} at a working voltage of 2.1 V *vs.* Li^+/Li°, with a large specific energy of 2600 W h kg^{-1}, assuming a complete reaction to Li_2S [6]. This value is 6.5 times that of the existing $LiCoO_2$/graphite system (~400 W h kg^{-1}) [7]. Sulfur, an abundant, cheap and less toxic material, is a promising choice as a high energy density cathode material for rechargeable lithium batteries. The use of sulfur as a cathode material does however pose problems, due to the high solubility of intermediate products (Li_2S_x, $4 \leq x \leq 8$) in commonly used liquid electrolytes [8], the large volume change between sulfur and Li_2S phases [7], and the insulating nature of sulfur, which leads to the use of low sulfur contents in cathode composites [9–12].

* Corresponding author. Tel.: +1 519 888 4567x35586; fax: +1 519 888 4347.
E-mail address: p4chen@uwaterloo.ca (P. Chen).

0378-7753/$ – see front matter © 2013 Elsevier B.V. All rights reserved.
http://dx.doi.org/10.1016/j.jpowsour.2013.04.113

To overcome these challenges, there have been several efforts focused on finding a host material, within which sulfur can be contained, to absorb polysulfides, provide conductive paths for electron transfer, and accommodate large volume change. There have been different approaches reported such as graphene-wrapping [13], hollow carbon nanofiber-encapsulation [7], multi-walled carbon nanotube addition [10,11,14], encapsulating sulfur into micropores or mesopores of carbon spheres [9,15], making composites with conductive polymers [14,16,17], mesoporous carbons [18,19], acetylene black [20], and graphene [21], using novel electrolytes [19,22,23], protection of lithium anode and cathode surfaces by coating conductive polymers [24,25]. Of all approaches, the sulfur/dehydrogenated polyacrylonitride (S/DPAN) composites have shown the best results both in terms of specific capacity and cyclability [14,16,26]. However, the reported sulfur contents are within 36–53 wt% [14,16,26,27], which are low and significantly decreases the specific energy of the composite. Therefore, identifying the maximum sulfur content that can be achieved in this composite system is important for further research and development in this direction.

The sulfur/dehydrogenated polyacrylonitrile composite system was first introduced by Wang et al. [16]. From X-ray photoelectron spectroscopy (XPS), Fourier transform infrared spectroscopy (FTIR) and Raman analysis, the authors concluded that sulfur is present in the elemental state (S_8) in the composite. Furthermore, they proposed a reaction scheme and suggested that the elemental sulfur is embedded in the heterocyclic ring of dehydrogenated PAN. However, Yu et al. [26] argued that elemental sulfur in the form of S_8 is too large to be embedded in the heterocyclic ring of DPAN. In view of these reports, we propose a more comprehensive binding scheme for the formation of S/DPAN composite, in which an 8 membered ring of sulfur embedded between 4 heterocyclic rings of dehydrogenated polyacrylonitrile. From the theoretical calculations and confirmed by experimental results, we show that the upper limit of sulfur content for the sulfur/dehydrogenated polyacrylonitrile composite, prepared from the mixture of polyacrylonitrile and excess sulfur, is 56 wt%. This indicates that whatever the effort to improve the electrochemical performance of this S/DPAN composite, the theoretical specific capacity of the composite is reduced to ~936 mA h g^{-1}. As a consequence, the maximum specific energy of the composite is ~1176 W h kg^{-1}, assuming a complete reaction to Li_2S at the average discharge potential of 1.8 V *vs.* Li^+/Li°. This specific energy is less than a half of the expected specific energy of a cathode consists of pure sulfur (~2600 W h kg^{-1}) [6]. This fact may serve as a criterion for the practical application of this composite as cathode material for lithium–sulfur batteries. Further increase of sulfur content will result in poor electrochemical performance, such as a reduced reversible capacity.

2. Experimental

2.1. Material preparation procedure

A sulfur (Sigma–Aldrich®, 100-mesh particle size) and PAN (Sigma–Aldrich®, average M_W = 150,000) mixture was ball milled (Fritsch, pulverisette 7) at a weight ratio of 4:1 for 5 h with ethanol as the dispersant. The resulting mixture was dried at 50 °C for 3 h in a vacuum oven and then annealed at 300 °C in argon. The heat treatment time was varied from 0.5 h to 4 h. Fig. S1 in Supplementary data shows the flow chart of preparation of the S/DPAN composites.

2.2. Material characterization

The crystalline phases of the samples were studied by X-ray diffraction analysis (XRD, D8 Discover, Bruker) equipped with Cu-Kα radiation, with a scan speed of 4° per minute ranging from 10° to 90°. The chemical transformation of the composites during the heat treatment process was investigated by Fourier transform infrared spectroscopy (FTIR, Bruker Tensor 27). The composite surface morphology was examined by field emission scanning electron microscopy (FE-SEM, Leo-1550, Zeiss) equipped with energy-dispersive X-ray spectroscopy (EDX, EDAX, Ametek Genesis V5.2). The particle size distribution, the calculation of geometric mean diameter $d_{g,p}$ and geometric standard deviation σ_g were done via a random sampling of particles from the FE-SEM images [28]. The interior structures of the samples were observed using transmission electron microscopy (TEM, CM10, Philips). The sulfur, carbon, hydrogen and nitrogen contents of the samples were analyzed using the elemental analyzer (CHNS, Vario Micro Cube, Elementar). The thermal decomposition behavior of the samples was determined by a thermogravimetry (TG)–differential thermal analysis (DTA) apparatus (TA instruments, Q-600). A temperature ramp mode at a heating rate of 10 °C min^{-1} was applied in a N_2 atmosphere.

2.3. Electrochemical measurements

The composite cathode comprised 80 wt% S/DPAN (or S/PAN) with 10 wt% ketjenblack (EC600JD, Akzo Nobel) and the rest was polyvinylidene fluoride (PVdF) (Kynar, HSV900) as the binder. These materials were dispersed in 1-methyl-2-pyrrolidinone (NMP, Sigma–Aldrich, ≥99.5% purity). The resultant slurry was spread uniformly onto a nickel foam disc (MTI, ≥99% purity) of 1 cm in diameter and ~800 μm in thickness. After drying in a vacuum oven at 50 °C for 12 h, the electrode was pressed at 8 MPa by a hydraulic presser in order to achieve a good contact between active material and nickel foam. The average weight of S/DPAN composite was ~10–12 mg per electrode (~12.7–15.3 mg cm^{-2}). The electrochemical performances of the S/DPAN composite samples were investigated using coin-type cells (CR2025). Each cell is composed of a lithium metal negative electrode and the S/DPAN composite positive electrode, separated by a microporous polypropylene film. 1 M $LiPF_6$ in a mixed solvent of ethylene carbonate (EC), dimethyl carbonate (DMC), and diethylene carbonate (DEC) with 1:1:1 weight ratio (LP71, Merck Chemicals) was used as the liquid electrolyte. The coin cells were assembled in a Braun glove box filled with high purity argon gas (99.9995% purity). The cells were tested galvanostatically on a multi-channel battery tester (BT-2000, Arbin) between 1 and 3 V at 0.2 C charge/discharge rate (current density = 334.4 mA g^{-1}). Applied currents and specific capacities were calculated on the basis of the weight of sulfur in the cathode. The cyclic voltammetry (CV) measurements were carried out using a multi-channel potentiostat (VMP3, Biologic). CV was performed between 1 and 3 V *vs.* Li^+/Li° at a scan rate of 0.1 mV s^{-1}. All electrochemical measurements were conducted at ~25 °C.

3. Results and discussion

In order to monitor the structural change during heat treatment, the variation of carbon/hydrogen (C/H) weight ratio and sulfur content was studied while varying heat treatment time from 0.5 to 4 h. S/DPAN-*X* (*X* = 0.5, 1, 1.5, 2, 2.5, 3, 3.5, 4 h of heat treatment time) were used to indicate the S/DPAN composites after different heat treatment times, and S/PAN was used to indicate the sample without heat treatment. The carbon, sulfur, nitrogen and hydrogen contents were identified by the elemental analysis. Fig. 1a represents the effect of the heat treatment time on carbon/nitrogen (C/N) and carbon/hydrogen (C/H) weight ratios in the composite. The C/N ratio remains constant, which was found to be about 2.57, corresponding to that of the PAN formula; thus PAN and its

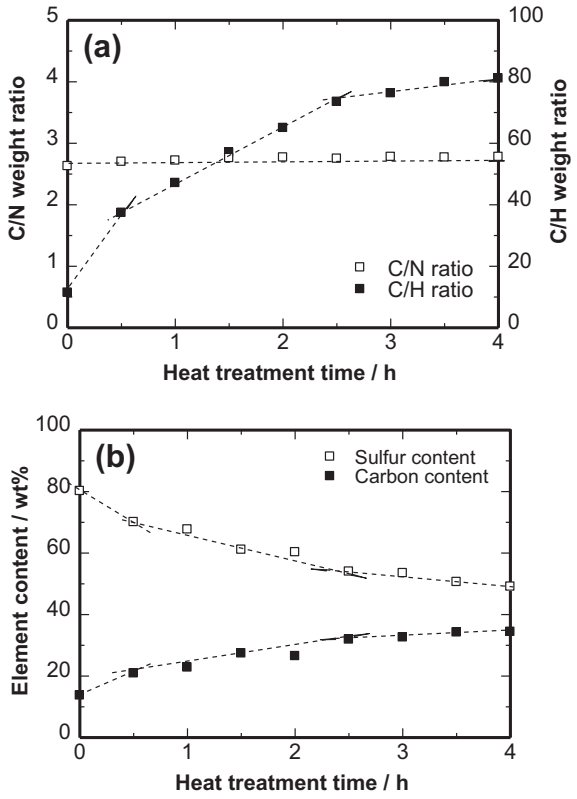

Fig. 1. Effect of heat treatment time on (a) C/N and C/H weight ratio, and (b) sulfur and carbon contents of the S/DPAN composites. The heat treatment time value of 0 h is used for the S/PAN sample after mixing by ball-milling. C/N, C/H weight ratios, sulfur and carbon contents were analyzed by elemental analysis.

dehydrogenated product have the same C/N ratio. For the C/H ratio, there are three stages may be assumed with respect to increasing heat treatment time. Before heat treatment, in each repeat unit of PAN, there are 3 hydrogen and 3 carbon atoms, causing the C/H ratio to be approximately 12, which is in agreement with the experimental result. During heat treatment, sulfur dehydrogenates PAN and H_2S is evolved, and the heterocyclic compound is formed. The number of hydrogen atoms in each repeat unit is reduced to 1, causing the C/H weight ratio to become ~36 [16]. This ratio is reached after about 0.5 h of heat treatment. The C/H ratio increases in the next 2 h at a lower rate, indicating another change in the dehydrogenation product. An interesting observation is that there is a change in the slope at heat treatment time of 2.5 h, after which the rate of increasing C/H becomes very small compared to the two earlier stages. The C/H ratio at this point is 73.5, indicating there are almost 6 atoms of carbon per atom of hydrogen in the composite.

Fig. 1b shows the sulfur and carbon contents of the composite during heat treatment. Again, three different stages are observed. In the first 0.5 h, the sulfur content decreases and the carbon content increases rapidly. This is in agreement with the results of the C/H ratio, and the relative increase in carbon content, by the removal of sulfur and hydrogen from the composite. Since the molecular weight of hydrogen is small in comparison to that of sulfur, the increase of carbon content mostly depends on the loss of sulfur. In the next 2 h, the sulfur content decreases at a lower rate, and after 2.5 h, the variation in sulfur and carbon contents become minimal. It was reported by Wang et al. [16] that the sulfur embedded in the composite is in elemental form. Considering the size of a cyclic sulfur molecule (S_8) [26], interesting information may be found. Elemental sulfur has a crown form ~4.4 Å in diameter; therefore it cannot be embedded in a heterocyclic ring of dehydrogenated PAN, which is ~2.5 Å in diameter. Considering the size, it was realized that a ring of sulfur is possibly embedded between 4 rings of the dehydrogenated PAN, and the C/H molar ratio is 6/1. Assuming this structure, the sulfur content should be $8\,M_S/(8\,M_S + 4\times 3\,M_C + 4\,M_N + 2\,M_H)\times 100 \approx 55.9$ wt% (M_x is the molar mass of the X element) and carbon content should be ~31.5 wt%. These are close to the experimental results after 2.5 h of heat treatment, which are 54.0 wt% of sulfur and 31.9 wt% of carbon. From 2.5 to 4 h, the sulfur content decreases and carbon content increases slightly to 49.1 wt% and 34.4 wt%, respectively, showing that after 2.5 h of heat treatment, a relatively stable structure has been formed, preventing the loss of sulfur through volatilization. Fig. 2a shows the reaction scheme of PAN and sulfur within the initial 0.5 h, similar to that illustrated by Wang et al. [16]. The heterocyclic structure is formed, in which the C/H molar ratio is 3 (C/H ratio weight is 36). Further dehydrogenation results in a C/H molar ratio of almost 6 as shown in Fig. 2b. One ring of sulfur may be trapped between 4 rings of the dehydrogenated PAN, leading to a much more stable configuration which showed insignificant change after further heat treatment. Moreover, the π electron of carbon atoms may contribute to a strong interaction (adsorption) between sulfur and carbon [26], which is responsible of lowering discharge voltage of composite from 2.1 to 1.8 V *vs.* Li^+/Li, and has been seen in sulfur cathode with encapsulated sulfur into nano-pores of carbon spheres [15].

Assuming the main weight loss in the composite is the loss of sulfur by either volatilization or reaction with hydrogen in PAN to form H_2S, using the carbon and sulfur content, as well as the C/H weight ratio, it is possible to find the weight loss percentage of sulfur attributed to each mechanism. Thus, sulfur loss during heat treatment from two main reasons can be monitored. The total weight loss percentage of sulfur can be derived from the sulfur content:

$$\Delta S_{\%}(t) = \left(1 - \frac{S(t)}{S_0}\right)100 \tag{1}$$

where S_0 is the sulfur content at the time $t = 0$, and

$$\Delta S_{\%}(t) = \Delta S_{\%}^{\mathrm{evap}}(t) + \Delta S_{\%}^{\mathrm{H_2S}}(t) \tag{2}$$

where $\Delta S_{\%}^{\mathrm{evap}}(t)$ and $\Delta S_{\%}^{\mathrm{H_2S}}(t)$ are the weight loss percentage caused by volatilization and H_2S formation, respectively. Since H_2S and

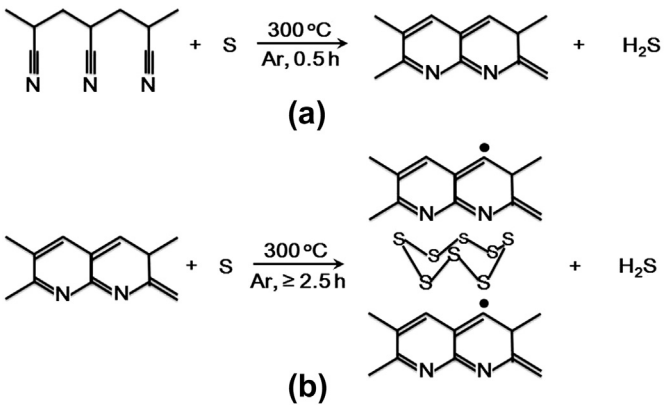

Fig. 2. The reaction schemes of PAN and sulfur after (a) 0.5 h and (b) 2.5 h of heat treatment at 300 °C in Ar atmosphere. Heating rate is 10 °C min^{-1} and the Ar flow rate is 150 mL min^{-1}. After 0.5 h, the C/H ratio is 3:1, which is the model proposed by Wang et al. [16]. However, after 2.5 h, the C/H ratio is 6:1, which suggests that 8-membered ring of sulfur was possibly embedded between 4 heterocyclic rings of the dehydrogenated PAN. The closed dots are the unbound electrons.

DPAN are the products of the dehydrogenation of PAN by sulfur [16], $\Delta S_{\%}^{H_2S}(t)$ can be found from the C/H ratio:

$$\Delta S_{\%}^{H_2S}(t) = \left(\frac{M_S}{2M_H} \left(\frac{1}{\frac{C}{H}(0)} - \frac{1}{\frac{C}{H}(t)} \right) \Big/ \left(\frac{S}{C}(0) \right) \right) 100 \quad (3)$$

where M_S and M_H are the molar masses of sulfur and hydrogen, respectively. According to these calculations, the weight loss of sulfur may be evaluated and is being presented in Fig. 3a. In the first stage, the loss of sulfur is very high by both mechanisms more than 40 wt% in total (compared to the final loss of 75 wt% in total). Even though the loss of sulfur by H_2S formation becomes less than 5 wt% in the second stage, the loss by volatilization is still significant (almost 25 wt%). The net loss of sulfur by volatilization is almost equal to the first stage. However when considering the time duration, the rate of volatilization in the second stage (2 h) is much smaller compared to that of the first stage (0.5 h) as shown in Fig. 3b. Finally the loss by reaction in the third stage is minor and the loss by volatilization is less than 5 wt% during 1.5 h of heat treatment. It is clear that forming the heterocyclic compound and attaining a suitable ratio of S/C may hinder sulfur volatilization.

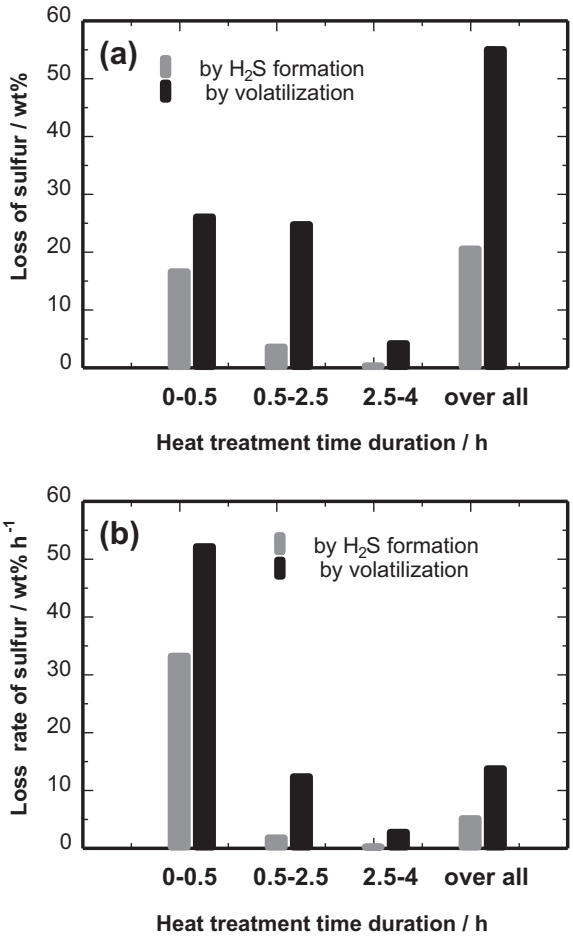

Fig. 3. The calculated (a) sulfur loss and (b) sulfur loss rate of the S/PAN composite (sulfur content is 80 wt%) during heat treatment at 300 °C in argon atmosphere at three different stages: 0 h–0.5 h, 0.5 h–2.5 h, 2.5 h–4 h and overall. The pale bars represent for the sulfur loss by reaction with hydrogen and the dark bars correspond to the sulfur loss by volatilization. Assuming the main weight loss in the composite is the loss of sulfur by either volatilization or H_2S formation, using the carbon and sulfur content as well as the C/H ratio, one can find the weight loss percentage of sulfur by one of the reasons.

Therefore, a heat treatment time of 2.5 h or longer is sufficient for the heat treatment process of the S/PAN system. The sulfur content ~56 wt% may be the upper limit for S/DPAN system.

To understand the crystallinity change of the composite during heat treatment, X-ray diffraction (XRD) patterns of all composite samples are shown in Fig. 4. The XRD patterns of sulfur and PAN as precursors are also presented. Although the ball milled S/PAN sample has a high crystalline pattern of sulfur, however no significant peak of PAN can be identified; which suggests an amorphous PAN phase is obtained after ball milling. By increasing the heat treatment time from 0.5 to 2 h, the crystallinity decreases. It is suggested by Wang et al. [16] that sulfur embedded among heterocyclic structures of dehydrogenated PAN leads to an amorphous phase, and crystal phases detected arise from the sulfur that is still outside of the embedded structure. When the heat treatment time is 2.5 h or greater, all samples were amorphous. This confirms the dehydrogenation of PAN by sulfur and sulfur embedding between the heterocyclic structures is nearly completed after 2.5 h of heat treatment and no more "free" sulfur is available for volatilization and H_2S formation.

In order to understand the physical and electrochemical property changes during heat treatment, four samples: S/PAN, S/DPAN-0.5 h, S/DPAN-2.5 h and S/DPAN-4 h were used for further characterization. Fig. 5 presents the FTIR spectra of PAN and the composites. The characteristic peak at 2244 cm^{-1} represents the −CN group, and the peak at 1455 cm^{-1} is related to the $-CH_2$ group, in the FTIR spectrum of PAN [16]. The spectra of S/PAN and PAN are similar, indicating that there is no chemical transformation of PAN during ball milling. After 0.5 h of heat treatment, these characteristic peaks no longer exist and are replaced by new peaks. The peak at 1498 cm^{-1} represents the C=C double bond. The formation of the cyclic structure is reflected in the peaks at 1427 cm^{-1} and 803 cm^{-1} [16]. The peak intensity significantly increases with heat treatment time from 0.5 to 2.5 h, and changes slightly when the heat treatment time increases from 2.5 to 4 h. This indicates that there is no significant chemical transformation between 2.5 and 4 h of heat treatment.

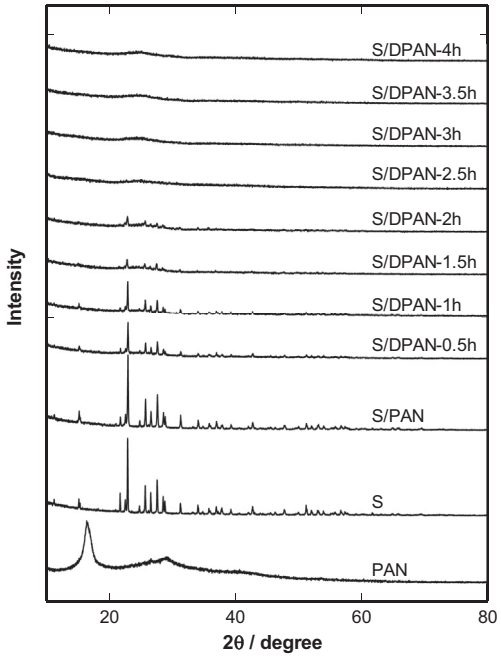

Fig. 4. XRD patterns of S, PAN and S/DPAN composites after different heat treatment times. Scanning speed is 4° min^{-1} using Cu-Kα detector.

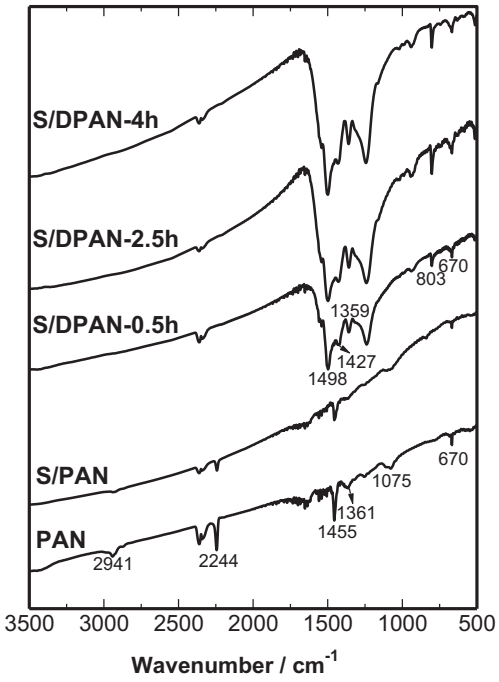

Fig. 5. FTIR spectra of PAN and the composites: S/PAN, S/DPAN-0.5 h, S/DPAN-2.5 h and S/DPAN-4 h.

The thermal behavior of the composites was studied. Fig. 6a shows the profiles of thermogravimetry (TG), time derivative of TG (DTG) and differential thermal analysis (DTA) of sulfur, PAN, and the composites with (S/DPAN-4 h) and without heat treatment (S/PAN). As can be seen in the DTA profile of sulfur, there are two endothermic effects occurring at around 115 °C and 300 °C, which are related to the melting and strong volatilization of elemental sulfur. Therefore, sulfur loss reaches a maximum at around 300 °C (DTG). This results in the loss of the entire mass as shown in its TG curve. On the other hand, according to the DTA profile of PAN, its decomposition occurs at approximately 290 °C, represented by an exothermic peak at that temperature. Between 290 °C and 500 °C, PAN loses about 60% of its initial weight. For the S/PAN mixture (sulfur content is 80 wt%) without heat treatment, the onset temperature of degradation (the temperature corresponding to 5% weight loss) is similar as that of the pure sulfur sample. In fact, their thermal behavior is identical except a weight loss step of less than 5% can be identified from 300 to 350 °C, corresponding to a small peak at about 350 °C in the DTG profile. This weight loss is attributed to the decomposition of PAN. Considering less than 25% weight loss of PAN (less than 5 wt% loss over 20 wt% of PAN in the S/PAN mixture) in comparison with 60% weight loss of the pure PAN, it is obvious that the interaction between sulfur and PAN creates a more stable structure. The small exothermic peak located near 340 °C represents the interaction between sulfur and PAN. Moreover, from DTG profiles, in the case of pure components and their mixture without prior heat treatment, sharp derivative peaks indicate an abrupt decomposition and degradation of the constituents. However, for the heat treated sample, a broad and low intensity peak shows a slow decomposition rate. This fact can also be confirmed in the DTA profile of S/DPAN-4 h composite where no obvious peak could be identified. It indicates that sufficient heat treatment time improves the thermal stability of the composites, which can be attributed to the formation of a relatively stable structure in the composites.

The thermal properties of four composites with different heat treatment times: S/PAN, S/DPAN-0.5 h, S/DPAN-2.5 h and S/DPAN-4 h are presented in Fig. 6b. With increasing heat treatment time, TG curves show that the total weight loss decreases. Furthermore, sharpness and intensity of the DTG peaks are reduced noticeably with increasing heat treatment time. This trend relates not only to smaller amounts of sulfur in the composites, but also the stability of the composites. The weight loss of S/PAN, S/DPAN-0.5 h, S/DPAN-

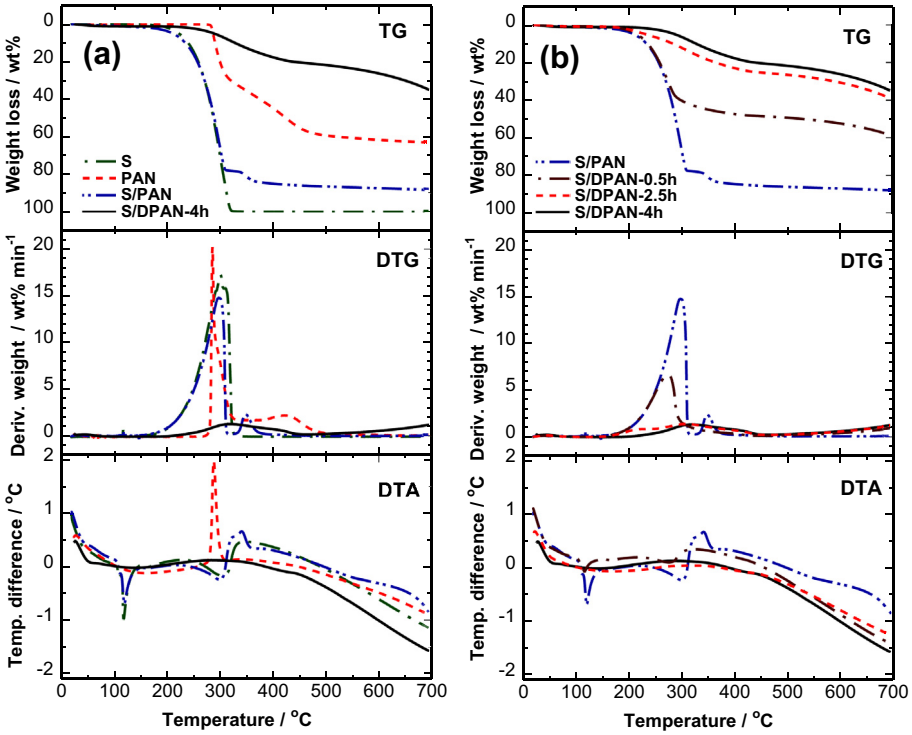

Fig. 6. TG, DTG and DTA profiles of (a) S, PAN and the composites with (S/DPAN-4 h) and without heat treatment (S/PAN) and (b) the composites with different heat treatment times: S/PAN, S/DPAN-0.5 h, S/DPAN-2.5 h and S/DPAN-4 h. A heating rate of 10 °C min^{-1} was applied for a temperature ramp mode in a N_2 atmosphere.

2.5 h and S/DPAN-4 h are 87, 58, 38 and 34%, respectively. However, the initial sulfur contents in S/DPAN-0.5 h, S/DPAN-2.5 h and S/DPAN-4 h were 70, 54 and 49 wt%, respectively. The weight losses are less than the initial sulfur contents in the heat treated composites, indicating that sufficient amounts of sulfur still remain in the final residues even after heating to 700 °C. The residues of S/DPAN-0.5 h, S/DPAN-2.5 h and S/DPAN-4 h were analyzed by elemental analysis. Despite of the difference in initial sulfur contents of the three composites, after TG experiment, all the residues have the same sulfur content of about 29 wt%, indicating that all residues have the same structure. The high sulfur contents of the residues after thermal analysis up to 700 °C emphasizes the strength of the composite matrix to retain elemental sulfur. The DTA profile of S/PAN-0.5 h shows the endothermic effects similar to S/PAN. It is clear that excess sulfur exists in this composite and is easily removed by the heating process. However, DTA curves of S/PAN-2.5 h and S/PAN-4 h are identical and have broadened low intensity peaks. This is a clear indication of improving thermal stability of the mixtures by increasing heat treatment time, with samples after heat treatment time of 2.5 h and 4 h showing almost the same thermal behavior.

Surface morphologies of the four samples: S/PAN, S/DPAN-0.5 h, S/DPAN-2.5 h and S/DPAN-4 h were observed by field emission scanning electron microscopy (FE-SEM), and their particle size distributions were calculated (see Figs. S2 and S3 in the Supplementary data). Even though morphologies of S/PAN and the S/DPAN samples are quite different, their geometric mean diameters, $d_{g,p}$, are almost similar within a range of 200–260 nm. There may be no further polymerization or depolymerization occurring during the heat treatment, except the cyclization of the repeat units of PAN. SEM images and their corresponding elemental (carbon, nitrogen and sulfur) mappings of the evaluated composites are shown in Fig. 7. Within the magnification range, the carbon, nitrogen and sulfur distributions are similar among 4 samples. It is noticed that sulfur seems to be distributed everywhere in the mapping. It may be because of the high sulfur content in the composite in comparison with carbon and nitrogen, and the sensitivity of the EDX detector which equipped with SEM. The sulfur mapping was reconfirmed by another EDX equipped with TEM, and it is obvious that sulfur is distributed uniformly within the interior structures of all the composites as shown in Fig. 8. This is because of the effect of the ball milling technique, however the uniformity in molecular scale is different. TEM observation (see Fig. S4 in the Supplementary data) shows that while the interior structure of S/PAN is heterogeneous, less significant phase separation can be identified in the S/PAN-2.5 h sample, indicating that the sulfur has been more

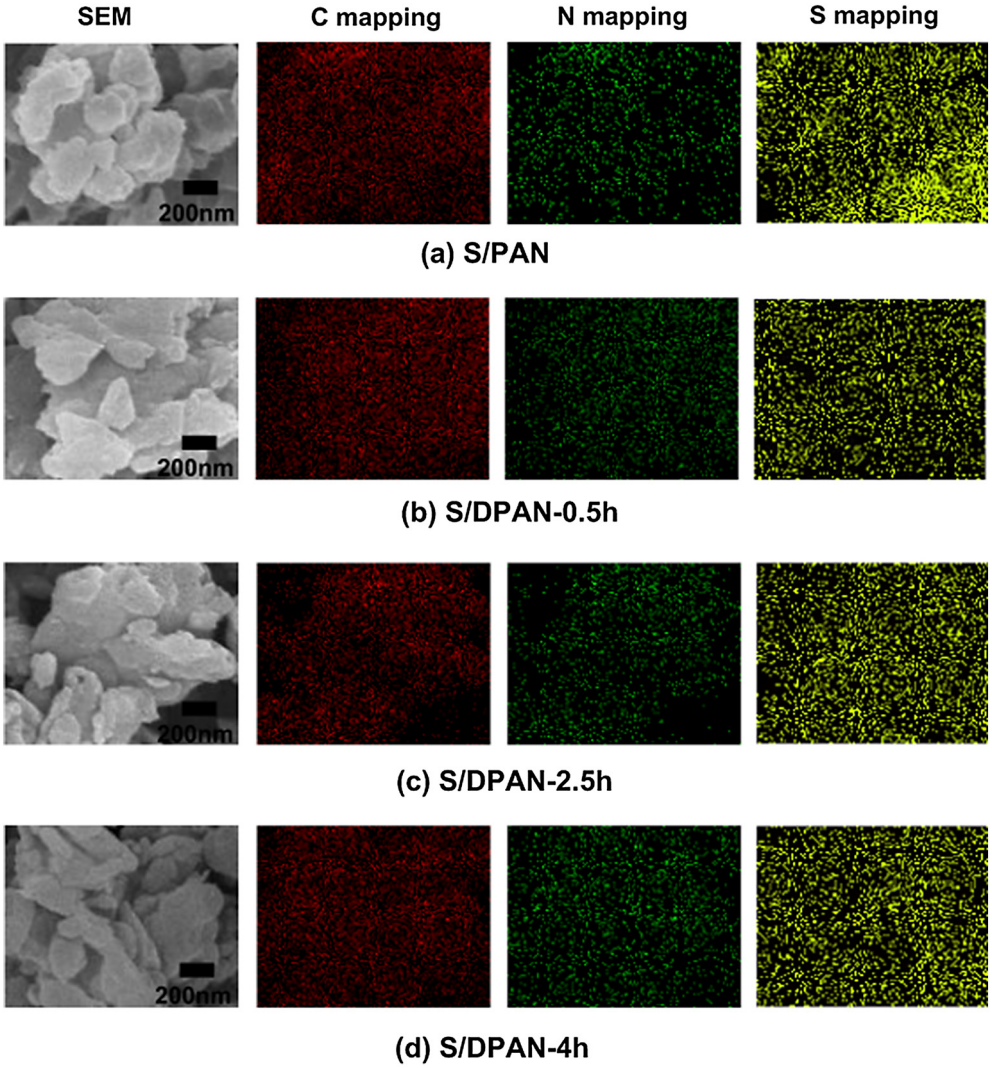

Fig. 7. Elemental mappings of the composites: (a) S/PAN, (b) S/DPAN-0.5 h, (c) S/DPAN-2.5 h and (d) S/DPAN-4 h.

uniformly distributed in the dehydrogenated PAN matrix after heat treatment. Nevertheless, due to the variation in other physical properties such as crystallinity (XRD), polymer structure (FTIR), thermal behavior (TG-DTA), the discharge–charge behavior of the cells containing these cathode materials is expected to be different.

From the investigation of physical properties of the composites, it can be concluded that heat treatment is vital in order to achieve a thermally stable S/DPAN system, where elemental sulfur is possibly embedded between 4 heterocyclic rings of the dehydrogenated PAN. It appears that 2.5 h is sufficient heat treatment time for completion of the dehydrogenation reaction of PAN and removing of all unbounded sulfur by volatilization. Further heat treatment slightly reduces the sulfur content without significant changing of the composite structure. The discharge–charge performance of the

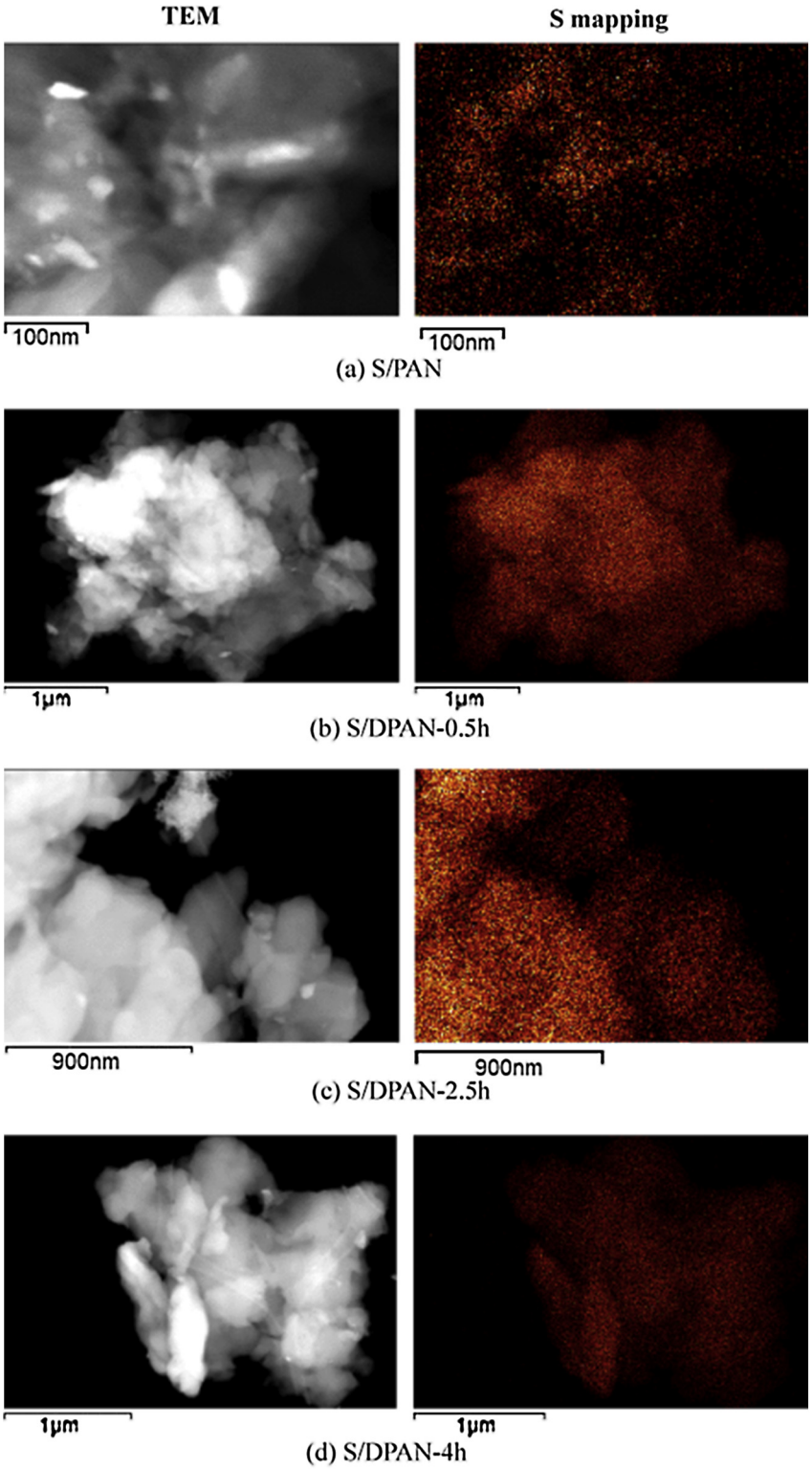

Fig. 8. TEM images and sulfur mappings of the composites: (a) S/PAN, (b) S/DPAN-0.5 h, (c) S/DPAN-2.5 h and (d) S/DPAN-4 h.

S/DPAN composites were characterized by using the coin type cells of Li | 1 M $LiPF_6$ in EC:DEC:DMC = 1:1:1 |S/DPAN. Fig. 9a presents the variation of specific discharge capacity at 5th cycle upon changing heat treatment time at 300 °C. While almost no discharge capacity can be delivered by the S/PAN, annealing it for 0.5 h resulted in a specific discharge capacity of 370 mA h g^{-1}. The specific discharge capacity increases slightly with the heat treatment time of up to 1.5 h, and then increases drastically with the heat treatment time up to 2.5 h. For the heat treatment times longer than 2.5 h, the specific discharge capacity decreased slightly. There might be slight deterioration in the S/DPAN structure with further heat treatment. It is confirmed that the annealing times of 2.5 h at 300 °C in argon atmosphere is sufficient in order to convert a mixture of sulfur and PAN (80 wt% of sulfur) into electrochemically active S/DPAN composites. The discharge–charge profiles of S/DPAN-0.5 h, S/DPAN-2.5 h and S/DPAN-4 h at the 5th cycle are presented in Fig. 9b. S/DPAN-2.5 h and S/DPAN-4 h samples exhibited flat charge and discharge plateaus around the 2 V region. It can be seen that the shape of discharge–charge profiles in the S/DPAN systems are different compared with those of elemental sulfur [8,22,24], and sulfur/carbon composite cathodes [7,13,25], which may result from the binding between sulfur and dehydrogenated PAN. S/DPAN-2.5 h and S/DPAN-4 h exhibited the specific discharge capacity between 950 and 1000 mA h g^{-1} at the 5th cycle. The irreversible capacities of the S/DPAN-2.5 h and S/DPAN-4 h samples are small (1.2% and 2.6% of the specific charge value for the S/DPAN-2.5 h and S/DPAN-4 h samples, respectively). On the other hand, the specific charge capacity of S/DPAN-0.5 h sample is about 70% of its specific discharge capacity at the 5th cycle. In addition, there is a large polarization loss between the charge and discharge plateaus of the S/DPAN-0.5 h. The S/PAN composite showed no electrochemical activity, confirming that appropriate heat treatment is vital in the synthesis of cathode material. Further electrochemical characterization of the S/DPAN-2.5 h was carried out. It is interesting to note that while the initial CV profile has 1 reduction peak in the publication of Wang et al. [16], there are 2 reduction peaks at 2.25 and 1.05 V *vs.* $Li^+/Li°$ in the first cycle of our CV profiles (see Fig. S5a in the Supplementary data). Some differences in preparation may lead to this variation. Nonetheless, the discharge–charge profiles in sequential cycles (see Fig. S5b in the Supplementary data) and the cyclability (see Fig. S6 in the Supplementary data) are similar to results in other publications of the S/DPAN system [16,26].

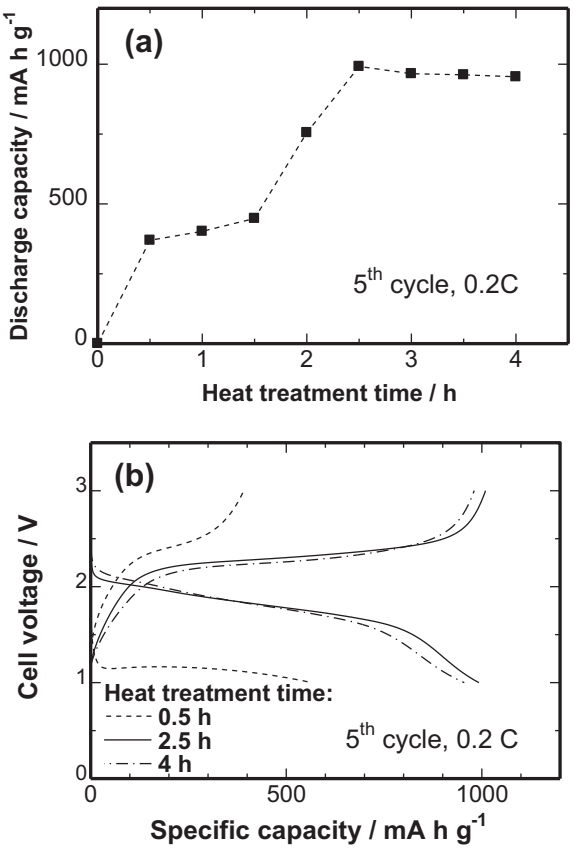

Fig. 9. (a) Effect of heat treatment time on the specific discharge capacities of the cells containing the S/DPAN composites at 0.2 C; (b) Discharge–charge profiles of the cells containing the composites: S/DPAN-0.5 h, S/DPAN-2.5 h and S/DPAN-4 h. All data was obtained at the 5th cycle. The discharge–charge rate is 0.2 C. The specific capacities were calculated based on sulfur weight.

4. Conclusions

Sulfur/dehydrogenated polyacrylonitrile composite is one of the most promising cathode materials for use in rechargeable lithium–sulfur batteries. However, the specific energy of this composite is not be as high as expected due to the low sulfur content in the composite according to reported results. Therefore, it is important to identify the upper limit of sulfur content that can be achieved while maintaining good electrochemical performance. To this end, the binding mechanism of sulfur and polyacrylonitrile should be elucidated. In this study, the heat treatment process was examined at varying timespans with excess sulfur. The results showed a constancy of sulfur content after a critical length of timespan, indicating the saturation of sulfur in the structure of dehydrogenated polyacrylonitrile. Based on molecular structure and size consideration, it is proposed that the principal feature of the binding mechanism involves the formation of an 8 membered ring of sulfur embedded between 4 heterocyclic rings of dehydrogenated polyacrylonitrile. This structural model and the experimental results indicated that the upper limit of sulfur content in the sulfur/dehydrogenated polyacrylonitrile composite is 56 wt%. Higher sulfur content will result in poor electrochemical performance, such as a reduced reversible capacity.

Acknowledgments

This research was financially supported by Positec, Natural Sciences and Engineering Research Council of Canada (NSERC), Canadian Foundation for Innovation (CFI) and the Canada Research Chairs (CRC) program. The authors would like to thank Dr. J. Byerley for assistance in editing the manuscript.

Appendix A. Supplementary data

Supplementary data related to this article can be found at http://dx.doi.org/10.1016/j.jpowsour.2013.04.113.

References

[1] M.S. Whitting Ham, Chem. Rev. 104 (2004) 4271–4301.
[2] R. Nagai, F. Kita, M. Yamada, H. Katayama, Hitachi Rev. 60 (2011) 28–32.
[3] A.K. Padhi, K.S. Nanjundaswamy, J.B. Goodenough, J. Electrochem. Soc. 144 (1997) 1188–1194.
[4] T. Ohzuku, M. Kitagawa, T. Hirai, J. Electrochem. Soc. 137 (1990) 769–775.
[5] Q. Zhong, A. Bonakdarpour, M. Zhang, Y. Gao, J.R. Dahn, J. Electrochem. Soc. 144 (1997) 205–213.
[6] J. Shim, K.A. Striebel, E.J. Cairnsa, J. Electrochem. Soc. 149 (2002) A1321–A1325.
[7] G. Zheng, Y. Yang, J.J. Cha, S.S. Hong, Y. Cui, Nano Lett. 11 (2011) 4462–4467.
[8] K. Kumaresan, Y. Mikhaylik, R.E. White, J. Electrochem. Soc. 155 (2008) A576–A582.

[9] X. Liang, Z. Wen, Y. Liu, H. Zhang, L. Huang, J. Jin, J. Power Sources 196 (2011) 3655–3658.
[10] L. Yuan, H. Yuan, X. Qiu, L. Chen, W. Zhu, J. Power Sources 189 (2009) 1141–1146.
[11] S.C. Han, M.S. Song, H. Lee, H.S. Kim, H.J. Ahn, J.Y. Lee, J. Electrochem. Soc. 150 (2003) A889–A893.
[12] X.L. Ji, K.T. Lee, L.F. Nazar, Nat. Mater. 8 (2009) 500–506.
[13] H. Wang, Y. Yang, Y. Liang, J.T. Robinson, Y. .Li, A. Jackson, Y. Cui, H. Dai, Nano Lett. 11 (2011) 2644–2647.
[14] W. Wei, J. Wang, L. Zhou, J. Yang, B. Schumann, Y. NuLi, Electrochem. Commun. 13 (2011) 399–402.
[15] B. Zhang, X. Qin, G.R. Li, X.P. Gao, Energy Environ. Sci. 3 (2010) 1531–1537.
[16] J. Wang, J. Yang, C. Wan, K. Du, J. Xie, N. Xu, Adv. Funct. Mater. 13 (2003) 487–492.
[17] M. Sun, S. Zhang, T. Jiang, L. Zhang, J. Yu, Electrochem. Commun. 10 (2008) 1819–1822.
[18] S.R. Chen, Y.P. Zhai, G.L. Xu, Y.X. Jiang, D.Y. Zhao, J.T. Li, L. Huang, S.G. Sun, Electrochim. Acta 56 (2011) 9549–9555.
[19] J. Wang, S.Y. Chew, Z.W. Zhao, S. Ashraf, D. Wexler, J. Chen, S.H. Ng, S.L. Chou, H.K. Liu, Carbon 46 (2008) 229–235.
[20] B. Zhang, C. Lai, Z. Zhou, X.P. Gao, Electrochim. Acta 54 (2009) 3708–3713.
[21] J.Z. Wang, L. Lu, M. Choucair, J.A. Stride, X. Xu, H.K. Liu, J. Power Sources 196 (2011) 7030–7034.
[22] J.W. Choi, G. Cheruvally, D.S. Kim, J.H. Ahn, K.W. Kim, H.J. Ahn, J. Power Sources 183 (2008) 441–445.
[23] S. Kim, Y. Jung, S.J. Park, J. Power Sources 152 (2005) 272–277.
[24] Y.M. Lee, N.S. Choi, J.H. Park, J.K. Park, J. Power Sources 119–121 (2003) 964–972.
[25] Y. Yang, G. Yu, J.J. Cha, H. Wu, M. Vosgueritchian, Y. Yao, Z. Bao, Y. Cui, ACS Nano 5 (2011) 9187–9193.
[26] X.G. Yu, J.Y. Xie, J. Yang, H.J. Huang, K. Wang, Z.S. Wen, J. Electroanal. Chem. 573 (2004) 121–128.
[27] J. Fanous, M. Wegner, J. Grimminger, Ä. Andresen, M.R. Buchmeiser, Chem. Mater. 23 (2011) 5024–5028.
[28] I. Taniguchi, Mater. Chem. Phys. 92 (2005) 172–179.